.

# Thermoelectric measurements using different tips in atomic force microscopy

S. S. Kushvaha, W. Hofbauer, Y. C. Loke, Samarendra P. Singh, and S. J. O'Shea

Citation: Journal of Applied Physics **109**, 084341 (2011); doi: 10.1063/1.3581073
View online: http://dx.doi.org/10.1063/1.3581073
View Table of Contents: http://aip.scitation.org/toc/jap/109/8
Published by the American Institute of Physics

# Thermoelectric measurements using different tips in atomic force microscopy

S. S. Kushvaha, W. Hofbauer, Y. C. Loke, Samarendra P. Singh, and S. J. O'Shea[a)]
*Institute of Materials Research and Engineering, A*STAR (Agency for Science, Technology and Research), 3 Research Link, Singapore 117602*

(Received 19 October 2010; accepted 19 March 2011; published online 27 April 2011)

We use conducting atomic force microscopy (AFM) in ultra high vacuum to measure the thermoelectric power of Au, Pt, and 3,4,9,10-perylene tetracarboxylic dianhydride (PTCDA) films. Tips coated with thick (1200 nm) Pt films or highly doped diamond film give reproducible data. The thermoelectric power of metal junctions formed with diamond tips is high but dominated by the diamond material thus making diamond tips of limited applicability in thermovoltage AFM. Pt coated tips on Au or Pt films gives small thermovoltage signal, making quantitative analysis of the thermopower on metal sample problematic. The thermovoltage AFM technique appears best suited to study organic thin films and the thermoelectric power of 1.5 nm and 2 nm thick PTCDA deposited on Au measured with Pt tips is −342 and −372 $\mu$V/K, respectively. The negative sign indicates that the lowest unoccupied molecular orbital level dominates electrical transport.
© *2011 American Institute of Physics*. [doi:10.1063/1.3581073]

## I. INTRODUCTION

Thermoelectric nanomaterials and films may play a key role in future thermoelectric devices for energy conversion or utilization.[1–3] The thermoelectric efficiency depends on the thermoelectric figure of merit $ZT = (S^2\sigma/k)T$, where $S$ is the thermoelectric power or Seebeck coefficient, $\sigma$ is the electrical conductivity, $k$ is the thermal conductivity and $T$ is the absolute temperature. Recently, scanning probe microscopy (SPM) methods have been developed to enable direct measurement of nanoscale thermoelectric properties.[4–9] Such localized measurements of $S$, $\sigma$, and $k$ can provide criteria to select new thermoelectric nanomaterials.

Another area of application for SPM is the measurement of local thermoelectric power of molecular heterojunctions, with an aim to elucidate electrical transport mechanisms in molecular electronic devices.[10] Specifically, if a temperature gradient is established across a SPM tip-sample junction, the measurement of the local thermovoltage signal generated at the junction can augment "standard" SPM methods, such as scanning tunneling microscopy (STM) and conducting atomic force microscopy (AFM). This is because, in comparison to STM and conduction AFM current−voltage ($I-V$) data, the thermovoltage signal is relatively insensitive to the number of molecules in the junction and can also determine if the lowest unoccupied or highest occupied molecular orbital (LUMO or HOMO) is closer to the Fermi level of the contacting metals.[11]

STM methods have previously been used to measure the local thermovoltage and electrical transport of various nanostructures and molecular interfaces.[4–6] However, STM techniques suffer from the problem that a bias voltage needs to be applied across the tip-sample gap to induce a tunneling current necessary for topography feedback (tip height) control. Thermovoltage, in contrast, is several orders of magnitude smaller than the STM bias voltage and should be measured in the absence of an electric current. These mutually incompatible regimes require switching between a tip height controlling state and a thermovoltage measuring state. This complicates the instrumentation and tip control, and the switching process is prone to introduce large transients and other electrical artifacts.

Since the tip contacts the surface to measure thermoelectric power, it is apparent that conduction AFM offers an alternative experimental approach, and recently Reddy *et al.* [8,9] demonstrated thermoelectric power measurements on a self-assembled monolayer using conducting AFM in ambient conditions. Related AFM based techniques have been used for mapping of thermal conductivity variations at the nanoscale,[12] thermopower profiling of a Si *p-n* junction,[13] and contact potential measurement between a heated conducting AFM tip and a metal film.[14] The principal advantage of AFM-based thermovoltage measurements is that topography feedback control is based on force measurements, and can therefore be performed independently of and simultaneously with electric measurements, eliminating several potential sources of artifacts.

An important issue in conducting AFM, and hence thermovoltage AFM, is to ensure the tip remains electrically conducting during an experiment, i.e., the tip must be robust.[15] In this paper we explore the use of different tips and present thermovoltage AFM data using conducting tips consisting of thick and thin Pt films, thin Au film, and conducting diamond films. As in conduction AFM[15] the tip can readily wear or oxidize, and our results on metal surfaces show that at present only diamond tips and thick Pt coated tips provide sufficiently repeatable thermovoltage AFM measurements. Both the diamond and thick Pt tips are rather blunt. Nevertheless, useful results were obtained on different

[a)]Author to whom correspondence should be addressed. Electronic mail: s-oshea@imre.a-star.edu.sg.

 © 2011 American Institute of Physics

metal surfaces and we also show thermovoltage data using thick Pt coated tips for thin film 3,4,9,10-perylene tetracarboxylic dianhydride (PTCDA), a material of interest for organic electronics.

## II. EXPERIMENT

Experiments were performed in contact mode in an RHK ultrahigh vacuum (UHV) AFM with a base pressure of $\sim 2 \times 10^{-10}$ Torr. The thermoelectric voltage was measured on samples consisting of evaporated Au and sputtered Pt films on mica, and PTCDA films on Au (111). All metal surfaces were degassed at 400 K for several hours in UHV to remove adsorbed gases and contamination. PTCDA films were grown by thermal evaporation on an evaporated Au (111) on mica surface at room temperature (RT) at a deposition rate of 0.01–0.03 nm/s in another high vacuum system, and quickly transferred to the UHV AFM system via a fast entry load lock chamber.

A schematic of the thermovoltage setup is shown in Fig. 1(a). A fast home-built electrometer amplifier is used to measure the output thermovoltage $V_{th}$ representing the thermoelectric signals ($\Delta V_1$, $\Delta V_2$, $\Delta V_3$) generated around the entire thermoelectric loop (Fig. 2). The different thermoelectric signals arise because temperature differences ($T_1$, $T_2$, $T_3$) exist across the tip and sample, and the surrounding ambient ($T_a$), as shown in Fig. 1(b). The input equivalent noise level of the amplifier is ~270 nV at a −3 dB bandwidth of 125 Hz, allowing fast recovery from overload that may occur due to an open circuit before the tip touches the sample. The metal substrate film of the sample is grounded. Shielded cabling (0.5 m) connects the amplifier to the conducting AFM cantilever. The AFM cantilever is kept at RT and the sample temperature is varied by supplying a heating current to a filament inside a metal sample holder. The sample is clamped onto a heat spreading copper disk, ensuring uniform temperature across the entire substrate. The sample temperature is measured using a thermocouple in contact with the copper disk.

In our experiments, we used a typical contact force of ~15 nN. The contact diameter of tip-metal junctions under plastic deformation conditions can be estimated as $d_{\text{plastic}} = (4\,F/\pi H_m)^{1/2}$, where $F$ is the contact force and $H_m$ is the hardness of the softer material. For $F = 15$ nN and $H_m$ ~100 MPa (for typical metals), the contact diameter is ~10 nm.[9,16] Similarly, if the contact is entirely elastic, the contact diameter under a Derjaguin-Muller-Toporov type load[17] is $d_{\text{elastic}} = [6R(F + F_c)/E^*]^{1/3}$where $R$ is the tip radius of curvature, $E^*$ is effective elastic modulus and $F_c$ is the tip-sample pull-off force (typically ~40 nN). The largest contact diameter expected in our experiments occurs for the softest sample (assuming $E^*$ ~1 GPa for PTCDA as found for self-assembled monolayers on Au)[18] probed with the largest tip ($R$ ~150 nm for a thick Pt coated tip), giving $d_{\text{elastic}}$ ~30 nm. Thus under typical conditions for both elastic and plastic deformation we expect the tip-sample contact diameter to be of order ~10 nm.

## III. TEMPERATURE DISTRIBUTION AND EFFECT ON MEASURED THERMOPOWER

While the quantity of interest in the experiment is the thermopower of the sample at the AFM tip-sample junction,

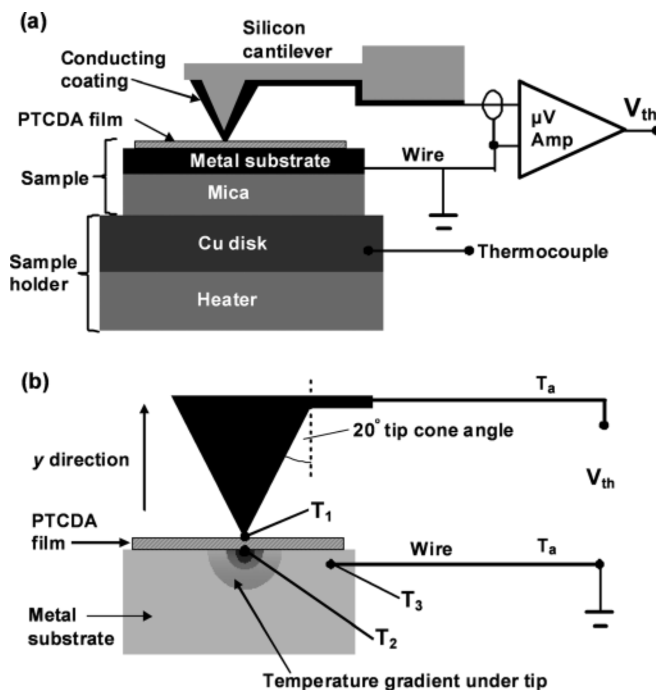


FIG. 1. (a) Schematic of the thermovoltage AFM measurement setup. Silicon cantilevers are used and the tips are coated with thick Pt or highly doped diamond films. The output voltage ($V_{th}$) is measured between the cantilever (at ambient) and a heated sample. In our experiments the sample is a metal film on mica, with PTCDA as an optional overlayer film. (b) Schematic view of the tip-sample contact showing temperatures defined in the analysis. $T_1$ is the temperature at the tip apex when in contact with the sample; $T_2$ is the temperature at the overlayer-metal substrate interface; $T_3$ is the temperature of the metal substrate, and is essentially the temperature measured by the thermocouple; and $T_a$ is the ambient temperature, which is the temperature of the wires at the input to the voltage amplifier. $T_1$, $T_2$, and $T_3$ differ because heat flows from the metal substrate to the tip in the region around the tip-sample contact.

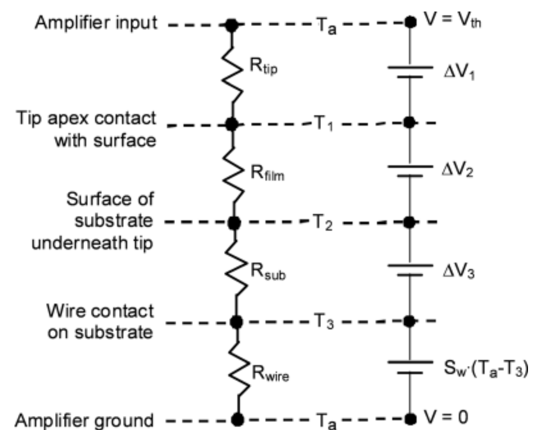


FIG. 2. (Left side) A schematic showing the thermal equivalent circuit used to determine the temperature ($T$) at various locations, based on the ratio of thermal resistances ($R$). (Right side) Electrical equivalent circuit, summing up thermovoltage contributions ($\Delta$V) arising from the temperature differentials and resulting in the thermoelectric output $V_{th}$ measured at the amplifier. Note that while the wire adds a contribution $S_w(T_a$-$T_3)$ to $V_{th}$, its thermal resistance $R_w$ does not affect the temperature distribution as it only appears as a thermal shunt between the heated sample and ambient.

this cannot be measured directly because the temperature gradient and concomitant thermovoltage is not confined to the tip-sample junction [Fig. 1(b) and Fig. 2]. In particular, the wiring that connects the sample to the reference input of the amplifier is exposed to the full temperature difference between sample and ambient, generating an additional thermovoltage that must be necessarily included in all measurements. The effective Seebeck coefficient of the wiring ($S_w$) was determined by a calibration experiment in which a bulk gold sample was brought into contact with a 0.2 mm diameter gold wire in lieu of the AFM tip. As the Seebeck coefficient of gold is well known,[19] the thermopower of the wiring can be readily determined from the observed total thermovoltage.

The temperature distribution along the tip-sample junction and, thereby, the individual thermoelectric contributions of tip and sample can be estimated using the heat diffusion equation, taking into account the geometry and thermal conductance of the AFM tip and sample. Below, we essentially follow earlier works[9,16,20] and adapt them to our specific experiment.

Referring to Fig. 2, the measured thermoelectric voltage is given as:

$$V_{\text{th}} = -S_W(T_3 - T_a) - S_{\text{sub}}(T_2 - T_3) - S_{\text{film}}(T_1 - T_2) - S_{\text{tip}}(T_a - T_1) = (T_3 - T_a)\left(\frac{(T_3 - T_2)}{(T_3 - T_a)}S_{\text{sub}} + \frac{(T_2 - T_1)}{(T_3 - T_a)}S_{\text{film}} + \frac{(T_1 - T_a)}{(T_3 - T_a)}S_{\text{tip}} - S_W\right), \quad (1)$$

where $S_w$, $S_{\text{tip}}$, $S_{\text{film}}$, and $S_{\text{sub}}$ are the Seebeck coefficients of the wire, tip, molecular film, and substrate, respectively.

By undertaking the experiment in vacuum, thermal leakage via air conduction/convection or liquid capillary formation is avoided, reducing the complexity of the thermal circuit; i.e., sample, film and tip are strictly connected in series. The steady-state temperatures $T_1$ and $T_2$ [Fig. 1(b)] can therefore be estimated by apportioning the applied temperature difference $T_3$ - $T_a$ according to the ratio of thermal resistances of AFM tip ($R_{\text{tip}}$), substrate ($R_{\text{sub}}$), and molecular film ($R_{\text{film}}$). The temperature $T_3$ is measured by the thermocouple. The overall thermoelectric voltage is then governed by a weighted sum of Seebeck coefficients

$$V_{\text{th}} = (T_3 – T_a)\left(\frac{R_{\text{tip}}}{R_{\text{tip}} + R_{\text{film}} + R_{\text{sub}}}S_{\text{tip}} + \frac{R_{\text{film}}}{R_{\text{tip}} + R_{\text{film}} + R_{\text{sub}}}S_{\text{film}} + \frac{R_{\text{sub}}}{R_{\text{tip}} + R_{\text{film}} + R_{\text{sub}}}S_{\text{sub}} - S_W\right). \quad (2)$$

The case of a direct tip-substrate contact (i.e. no PTCDA film) is included in this expression by setting $R_{\text{film}} = 0$ (which implies $T_1 = T_2$).

We have obtained the various thermal resistances ($R_{\text{sub}}$, $R_{\text{tip}}$, $R_{\text{film}}$) from the heat diffusion equation $j = -k\nabla T$ for a given geometry,[9,16,20] where $j$ is the heat flux density and $k$ the local thermal conductivity. The stationary heat flow through a nanocontact of diameter $d$ on a planar bulk substrate with heat conductivity $k_{\text{sub}}$ can be approximated by a semi-spherical geometry, associated with a thermal resistance of[16]

$$R_{sub} = \frac{1}{\pi k_{\text{sub}} d}. \quad (3)$$

The thermal resistance of different metal substrates is calculated for bulk values of thermal conductivities of Pt and Au.[21]

The thermal resistance of a coated silicon AFM tip, neglecting lateral heat flow, can be approximated by integration along the tip vertical axis $y$ as[16]

$$R_{tip} = \int_0^H \frac{dy}{A_{\text{Si}}(y)k_{\text{Si}} + A_{\text{coat}}(y)k_{\text{coat}}}, \quad (4)$$

where $H$ is the total tip height, $A(y)$ is the cross section at tip height $y$, and $k$ is the thermal conductivity. The subscripts refer to the contributions by silicon ("Si") and the conductive coating ("coat"). To obtain the respective cross sections, we model the tip geometry as a silicon cone covered with a uniform coating layer (i.e., Pt or diamond) of a given thickness, truncated to a contact area of diameter $d$. While an analytical solution of the above expression exists for this geometry, it is rather unwieldy, and we resorted to numerical integration. The thermal resistance of coated tips is given in Table I for different thermal conductivities of Pt and diamond.[21,22]

For the molecular film, if the thickness $t$ of the film is small compared to the contact size $d$, lateral heat flow components (edge effects) may be neglected, and the associated thermal resistance is

$$R_{film} = \frac{4t}{\pi d^2 k_{\text{film}}}, \quad (5)$$

where $k_{\text{film}}$ is the thermal conductivity of the film [$k_{\text{film}}$ for PTCDA ~10 W/(m·K)].[23]

The calculated thermal resistances are summarized in Table I. It should also be noted that the temperature gradient is mostly confined to a small volume around the tip-sample contact, and uncertainties of the nanoscale geometry of the contact region may have disproportionate effects on the thermal resistances. We also ignored the temperature drop along the AFM cantilever. We validated this assumption by measuring the resonance frequency of the cantilever, which changed by about -100 ppm when the sample was heated from 298 to 393 K. Using the known temperature coefficient (−30 ppm/K) of the resonance frequency,[24] this translates to a 3% effect which is negligible compared to other uncertainties (e.g., the geometry of the tip-sample contact).

## IV. RESULTS AND DISCUSSION

### A. Thermoelectric power of Au and Pt films

Various conducting tips were prepared to measure the thermoelectric power of junctions formed by conducting AFM tips and thin Au and Pt films. For each tip, measurements were repeated ~50 times, contacting the sample in different locations, and experimental errors are estimated from the spread of this data. Where several different tips were used on the same type of sample, consistent results were obtained. A summary of all measurements, including a calibration measurement of a bulk gold wire touching a bulk

TABLE I. Estimated thermal resistances of AFM tips, substrates, and PTCDA molecular films based on the following parameters. AFM tip geometry: height $H = 15$ μm; cone semi-angle $\theta = 20°$; contact diameter $d = 10$ nm; Pt coating thickness $t_{Pt} = 150$ nm; diamond coating thickness $t_{dia} = 100$ nm. Thermal conductivities (at 300 K): $k_{Au} = 317$ W/(m·K);[21] $k_{Pt} = 71.6$ W/(m·K);[21] $k_{Si} = 148$ W/(m·K);[21] $k_{dia} = 1000$ W/(m·K);[21,22] $k_{PTCDA} = 10$ W/(m·K).[23]

| Component | Thermal resistance $R_{th}$ [$10^5$ K/W] |
|---|---|
| Pt coated Si AFM tip | 24.2 |
| Diamond coated Si AFM tip | 1.8 |
| Au substrate | 1.0 |
| Pt substrate | 4.5 |
| PTCDA film (1.5 nm) | 19.1 |
| PTCDA film (2 nm) | 25.5 |

gold sample (to determine $S_w$), is given in Table II and discussed below.

Initially, conducting tips were made by sputtering 50 nm of Au or Pt on Si AFM probes. However, these thin film coated tips were found to be unsuitable for stable and repeatable thermovoltage AFM measurements (data not shown). Current−voltage ($I-V$) curves at low bias show the metal film wears rapidly from the tip apex and the tip becomes nonconducting. To obtain more stable probes, thick Pt film tips were produced by sputtering 1200 nm of Pt onto the Si tips. This considerably blunts the tips (radius of curvature $R_{tip}$ ∼150 nm, determined from scanning electron microscopy micrographs) but ensures the tips remain robust and allow repeatable thermovoltage measurements. Typical data using the thick Pt coated tip on a Pt substrate is shown in Fig. 3(a), with the measured thermovoltage changing linearly with the sample-ambient temperature difference. To eliminate the effects of any offset voltages, the thermoelectric power is determined from the average slope of this graph, under the premise that any dependence of Seebeck coefficients on temperature is small. This assumption is justified given that the uncertainties in measurement and analysis are comparable to any nonlinearity in the data.

As observed in previous work,[9] the magnitudes of the observed Seebeck coefficients are significantly smaller than one would expect from the bulk values of the materials forming the junctions. In the special case of a Pt coated tip on a Pt sample, we can eliminate the uncertainty associated with the distribution of the applied temperature difference by treating the tip-substrate junction as a homogeneous material. Under this assumption, we obtain a value of $S_{Pt} = -1.86$ μV/K (Table II), which is only about third of the reported bulk value of −5.28 μV/K.[19] A possible explanation may lie in the structure of the Pt film and coating. The sputtered films have a rather small grain size of ∼20 nm (estimated from STM and SEM imaging, not shown), which may significantly affect transport properties. In a study on thin film thermocouples,[25,26] a comparable reduction in thermopower of a Pt film was demonstrated and attributed to the film thickness limiting the electron mean free path in one dimension. The granular structure of sputtered Pt films would restrict the mean free path in all three dimensions, and may even enhance this effect. This observation of lowered thermopower highlights a potential difficulty in scanning probe thermovoltage measurements, as the preparation of the probe may have unexpectedly large effects on the experiment.

In the case of a Pt coated tip in contact with an Au film, we do not have a quantitative explanation for the observed thermopower, despite excellent reproducibility of the measured thermoelectric response using several tips. Specifically, if $S_{tip}$ is taken as −1.86 μV/K (i.e., as found in the Pt on Pt experiments) we find $S_{sub} = 43.5$ μV/K for Au substrate, which is clearly not realistic. Possibly the Au substrate introduces further thin film effects restricting the electron mean free path, but we note that these evaporated and annealed Au(111) films have a large lateral grain size, on the order of hundreds of nanometers. More probably the problem arises from large uncertainties in the calculations. We notice that the thermal resistance of the Pt tip, estimated from the bulk thermal conductivity, is significantly larger than that of the Au substrate; hence, the expected temperature drop across the substrate is very small (4%). Given the measurement uncertainties, the relatively small value of $(T_2-T_1)$ makes analysis difficult and the errors large. Further uncertainty arises because the small grain size of the sputtered Pt may

TABLE II. Measured thermoelectric response for different substrate/film/tip combinations, estimated distribution of the applied temperature gradient (in %), and calculated Seebeck coefficients (all in μV/K). Probes are Si tips coated with a layer of Pt, Au, or highly *p*-doped diamond. Evaporated Au and sputtered Pt films are 50 nm thick. The Seebeck coefficient of Au (boldface) is taken from the literature[19] and used as a reference. The Au (bulk) substrate/Au (bulk) tip experiment was used to find the thermopower of the wires ($S_w$) connecting to the sample. The calculated value of $S_{sub}$ marked with * for the Pt tip-Au combination is shown for completeness but is clearly not realistic. The uncertainty in the thermoelectric power at each value of sample-ambient temperature difference, as shown by the error bars in Figs. 3 and 5, was estimated from the total spread of repeated measurements ($n \sim 50$) using a given tip. The error in the voltage vs. temperature slope was found by manually fitting the data curves.

| Substrate | Film | Tip | No. of tips used | Measured Thermoelectric response (μV/K) | % sub | % film | % tip | $S_{sub}$ μV/K | $S_{film}$ μV/K | $S_{tip}$ μV/K | $S_w$ μV/K |
|---|---|---|---|---|---|---|---|---|---|---|---|
| Au (bulk) | — | Au (bulk) | 1 | +0.5 ± 0.2 | — | — | — | **1.94** | — | **1.94** | 1.44 |
| Pt | — | Pt | 1 | −3.3 ± 0.2 | — | — | — | −1.86 | — | −1.86 | 1.44 |
| Au | — | Pt | 3 | −1.5 ± 0.2 | 4 | — | 96 | 43.5* | — | −1.86 | 1.44 |
| Pt | — | diamond | 2 | + 20 ± 2 | 71 | — | 29 | −1.86 | — | 80 | 1.44 |
| Au | — | diamond | 3 | + 15 ± 2 | 36 | — | 64 | **1.94** | — | 25 | 1.44 |
| Au | PTCDA (1.5 nm) | Pt | 2 | −140 ± 10 | 2 | 43 | 55 | **1.94** | −342 | −1.86 | 1.44 |
| Au | PTCDA (2 nm) | Pt | 2 | −190 ± 20 | 2 | 50 | 48 | **1.94** | −372 | −1.86 | 1.44 |

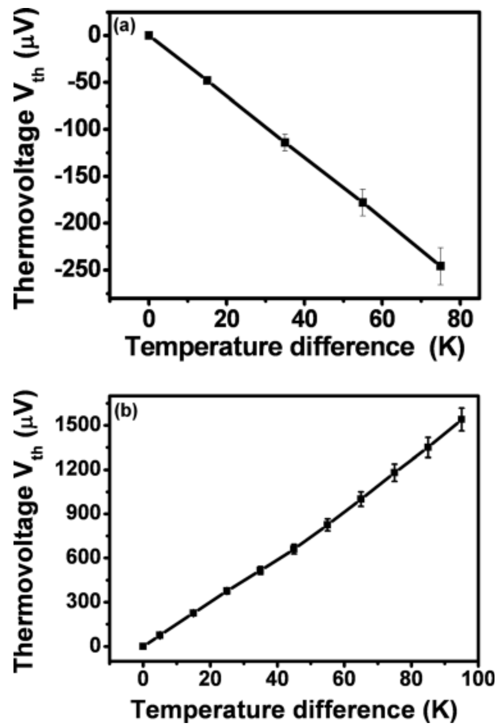


FIG. 3. Plot of the measured thermovoltage output ($V_{th}$) vs sample-ambient temperature difference for: (a) 50 nm thick Pt film on mica using a thick Pt coated tip; (b) 50 nm thick Au film on mica using a highly doped (*p*-type) diamond coated tip.

also significantly affect the thermal conductivity of the tip, invalidating temperature distribution estimates.

The above results illustrate that, for practical thermovoltage measurements, it is desirable to minimize the thermal resistance of the probe so as to confine the temperature gradient on the sample of interest rather than on the probe. Doped (conducting) diamond coated AFM tips are promising in this respect due to the excellent heat conductance of diamond [$k = 1000$ W/(m·K)].[21,22] Indeed, a large thermoelectric response is seen with diamond tips on Pt and Au substrates [Table II and Fig. 3(b)], with the positive value of $S_{tip}$ confirming the *p*-type doping of the diamond. However, despite the reduced temperature drop across the tip, the large Seebeck coefficient associated with doped diamond overwhelms the thermovoltage contribution of the metallic samples, making extraction of the Seebeck coefficients of the sample impractical. As an additional difficulty for reliable thermovoltage characterization using diamond tips, the Seebeck coefficient for the probes may be variable due to differences in doping. Values in the range of 300 to 600 $\mu$V/K have been reported elsewhere for doped diamond films,[27] whereas in our experiments we estimate the Seebeck coefficient for the diamond tips to be 25 to 80 $\mu$V/K.

Irrespective of the difficulty in finding the Seebeck coefficient for the diamond tips, the value of $S_{tip}$ is still more than an order of magnitude larger than $S_{sub}$ of typical metallic samples, making it difficult or impractical to extract the sample thermopower. Clearly, metallic probes with their smaller intrinsic thermopower are more desirable. Figure 4 shows schematically the issues encountered using diamond or Pt AFM tips. To extract the thermovoltage of the substrate

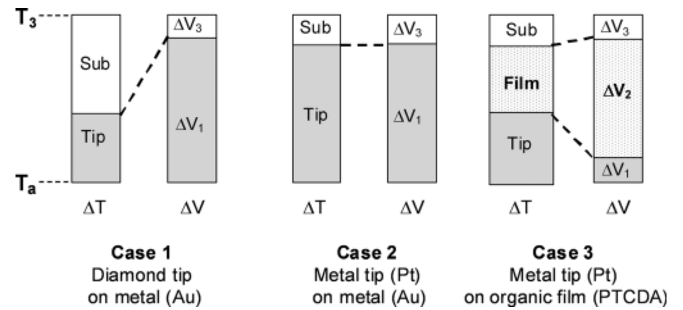


FIG. 4. Schematic showing the relative weighting of the temperature ($\Delta T$) and thermovoltage ($\Delta V$) drops across the tip region (the shaded area labeled "tip" and $\Delta V_1$) and substrate (the clear area labeled "sub" and $\Delta V_3$) for three different tip-substrate combinations. In case three an additional temperature and voltage drop is present ($\Delta V_2$) arising from the presence of a PTCDA film.

($\Delta V_3$) it is preferable, given all the experimental and analysis uncertainties, to have a much smaller voltage drop over the tip ($\Delta V_1$) i.e., we require $\Delta V_1 \ll \Delta V_3$. In case 1 (diamond tip on metal) this condition is not met because although the temperature drop $\Delta T$ across the tip is smaller than the metal substrate, the much larger Seebeck coefficient of the diamond results in $\Delta V_1$ being much larger than $\Delta V_3$. Conversely in case 2 (Pt tip on Au) the Seebeck coefficients are of the same orders but here most temperature drop $\Delta T$ occurs across the tip and again $\Delta V_1 \gg \Delta V_3$. In case 3, discussed below, a molecular film of PTCDA separates a metal tip from a metal substrate. In this case sufficient temperature drop occurs across the film and the film has high thermopower; hence a large thermovoltage is generated across the film ($\Delta V_2$) allowing useful thermopower data to be obtained on the film.

### B. Thermoelectric power of PTCDA film using Pt tip

The robustness and small Seebeck coefficient of the thick Pt coated tips makes them useful for obtaining meaningful data for some technologically interesting surfaces. The problem in the experiments on metal films was the comparatively low thermal conductivity of the tip. The effect of temperature drops across the probe becomes less significant for samples that are poor thermal conductors themselves, e.g. organic films. Fig. 5 shows an example using data for PTCDA films grown on Au (111). At the low coverages used, the surface comprises two regions [Fig. 5(a)]; regions where one or two monolayers lie flat on the Au surface, and thicker regions where the PTCDA molecules still lie parallel to the surface but grow as islands.[28] The measured thermoelectric response of the Pt-PTCDA-Au junctions is ($-140 \pm 10$) $\mu$V/K for 1.5 nm thick PTCDA and ($-190 \pm 20$) $\mu$V/K for 2-nm thick PTCDA [Figs. 5(b) and 5(c)]. Based on the estimated temperature distribution, this translates to PTCDA Seebeck coefficients (see Table II) of $-342$ $\mu$V/K (1.5 nm film) and $-372$ $\mu$V/K (2 nm film). These values are much larger in magnitude than the thermoelectric power measured for all-metal junctions, and such behavior is expected for organic materials where the hybridized electronic structure closely approaches the discrete molecular energy levels.[10,29] In general, the thermoelectric response is dominated by the molecular orbital (HOMO or LUMO) energetically closest to the Fermi level, determining the sign of the Seebeck coefficient.[6,8,11] The

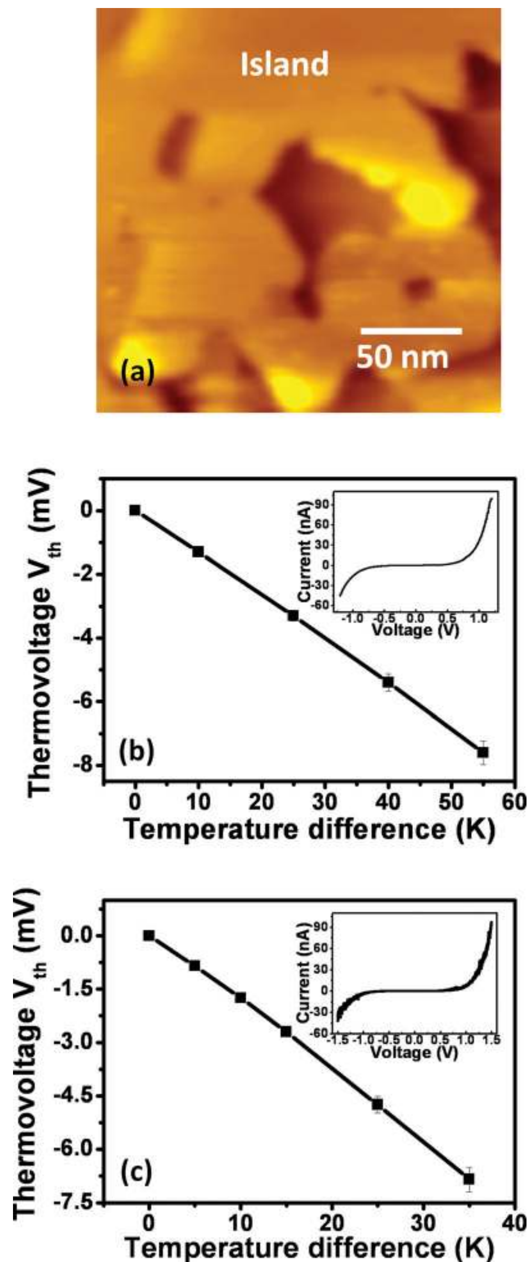


FIG. 5. (Color online) (a) A tapping mode AFM image of a PTCDA film on Au. The bright to dark contrast represents a sample height of 1.5 nm. Thermovoltage measurements are done on the island regions. Plots of the measured thermovoltage output ($V_{th}$) vs sample-ambient temperature difference are shown for (b) 1.5-nm and (c) 2-nm PTCDA films grown on Au(111) using thick Pt-coated tips. The insets show $I-V$ curves on the PTCDA taken in contact mode using the same tips.

negative thermoelectric power for Pt-PTCDA-Au junction demonstrates that $n$-type conductivity is dominating for PTCDA grown on Au, i.e., the Fermi level is closer to the LUMO.

The magnitude of the thermoelectric power increases slightly as the film becomes thicker (from $-342$ to $-372$ $\mu$V/K). A Seebeck coefficient of $-1100$ $\mu$V/K for a 50 nm thick PTCDA film has also been reported previously.[29] These two measurements indicate that the thermoelectric power of PTCDA on Au may depend on the thickness of the film. We also measured current$-$voltage ($I-V$) curves of PTCDA films on Au (111) with Pt coated AFM tips in contact mode, as shown in the insets of Figs. 5(b) and 5(c). The $I-V$ curves are asymmetric with higher conductivity at positive compared to negative sample bias. Previous scanning tunneling spectroscopy (STS) studies of PTCDA grown on Au(111) revealed that the LUMO level of several monolayers of PTCDA is $+$ 1.0 V above the Fermi level, whereas the HOMO level is $-1.9$ V below the Fermi level.[30] Our $I-V$ data qualitatively shows that the HOMO-LUMO gap of 2 nm thick PTCDA is larger than that of 1.5 nm thick PTCDA. A possible explanation for this thickness dependence of the HOMO-LUMO gap, which correlates with the observed thickness dependence of the thermoelectric power, is that the energy levels of organic molecules on or near a metal surface are shifted due to image charge/surface polarization effects.[31] The observed HOMO-LUMO gap depends thus on the thickness of the film between the metal electrodes, approaching a constant, asymptotic value only for sufficiently thick films where such interface effects are negligible.[31] However, a quantitative description of the measured thickness dependence of the thermoelectric power for PTCDA requires an atomic level model for the Pt-PTCDA-Au junction.

## V. CONCLUSION

In summary, we employed conducting AFM in UHV to measure the thermoelectric power of 50 nm Au and 50 nm Pt films on mica and PTCDA films on Au. Highly doped $p$-type diamond and thick (1200 nm) Pt coated Si tips were found to be sufficiently robust for reproducible thermovoltage experiments in contact AFM mode. Tips coated with thin (50 nm) Au or Pt coatings were found to be unsatisfactory because the conducting coatings wear off the tip apex.

The thermoelectric power of a junction using a thick Pt coated probe and a Pt film resulted in markedly diminished Seebeck coefficients compared to bulk value.[19] We suggest that the discrepancy may arise from the grain structure of the sputtered metal films limiting the electron mean free path. Such effects might also affect other transport properties, i.e., thermal conductance, and this lead to considerable measurement uncertainty due to the variability of tip properties. This may point to a general difficulty for thermoelectric measurements on the nanoscale, in that the probe properties may differ considerably from the known bulk values. In the case of a thick Pt tip on a Au film, the thermal resistance of the probe dominates over that of the sample, making a quantitative analysis of the sample's thermopower impractical and highlighting the need for high thermal conductance of the probe.

Conducting (doped) diamond probes have low thermal resistance, but their large Seebeck coefficients were found to overwhelm the thermopower of metallic samples. Such tips may be suited for measuring samples with large intrinsic thermopower; however, the strong dependence of the diamond Seebeck coefficient on varying doping levels, and uncertainties in thermal conductivity and tip geometry due to the polycrystalline structure of the film, may still introduce considerable error. Thus it appears that diamond tips have limited applicability in thermovoltage AFM.

Thick Pt coated tips were found to be suitable for measuring the thermoelectric response of a PTCDA molecular film in a Pt-molecule-Au junction. The measured Seebeck coefficient is large and has negative sign, indicating *n*-type behavior with electronic transport being dominated by the LUMO. There are indications that the thermoelectric power of Pt-PTCDA-Au junctions depends on the PTCDA thickness, which we attribute to surface polarization effects. This interpretation is supported by *in situ* $I-V$ spectroscopy using the same Pt tip.

The advent of thermovoltage AFM to measure local thermoelectric power will help investigate nanomaterials for future thermoelectric devices and molecular electronics.[6,8] However, as in conduction AFM,[15] there is still a major challenge to fabricate probes that are sufficiently sharp, sufficiently robust, and sufficiently uniform or characterized. Beyond these attributes, good thermovoltage probes also require high thermal conductivity and small intrinsic thermopower, both of which may be difficult to predict from bulk properties and depend on the fabrication process.

## ACKNOWLEDGMENTS

The authors would like to thank Professor Chandrasekhar Natarajan for useful discussion and Dr. Ramesh Thamankar, K. Shubhakar and Qin Hailang for technical support and discussions.


[1] T. C. Harman, P. J. Taylor, M. P. Walsh, and B. E. LaForge, Science **297**, 2229 (2002).
[2] R. Venkatasubramanian, E. Siivola, T. Colpitts, and B. O'Quinn, Nature **413**, 597 (2001).
[3] A. I. Hochbaum, R. Chen, R. D. Delgado, W. Liang, E. C. Garnett, M. Najarian, A. Majumdar, and P. Yang, Nature **451**, 163 (2008).
[4] J. C. Poler, R. M. Zimmermann, and E. C. Cox, Langmuir **11**, 2689 (1995).
[5] H.-K. Lyeo, A. A. Khajetoorians, L. Shi, K. P. Pipe, R. J. Ram, A. Shakouri, and C. K. Shih, Science **303**, 816 (2004).
[6] P. Reddy, S. Y. Jang, R. A. Segalman, and A. Majumdar, Science **315**, 1568 (2007).
[7] J. A. Malen, P. Doak, K. Baheti, T. D. Tilley, R. A. Segalman, and A. Majumdar, Nano Lett. **9**, 1164 (2009).
[8] A. Tan, S. Sadat, and P. Reddy, Appl. Phys. Lett. **96**, 013110 (2010).
[9] S. Sadat, A. Tan, Y. J. Chua, and P. Reddy, Nano Lett. **10**, 2613 (2010).
[10] J. R. Heath, Annu. Rev. Mater. Res. **39**, 1 (2009)
[11] M. Paulsson and S. Datta, Phys. Rev. B **67**, 241403(R) (2003).
[12] M. Nonnenmacher and H. K. Wickramasinghe, Appl. Phys. Lett. **61**, 168 (1992).
[13] K. Kim, J. Park, S. U. Kim, O. Kwon, J. S. Lee, S. H. Park, and Y. K. Choi, Appl. Phys. Lett. **90**, 043107 (2007).
[14] J. L. Remmert, Y. Wu, J. Lee, M. A. Shannon, and W. P. King, Appl. Phys. Lett. **91**, 143111 (2007).
[15] M. A. Lantz, S. J. O'Shea, and M. E. Welland, Rev. Sci. Instrum. **69**, 1757 (1998).
[16] A. Majumdar, Annu. Rev. Mater. Sci. **29**, 505 (1999).
[17] B. V. Derjaguin, V. M. Muller, and Y. P. Toporov, J. Colloid Interface Sci. **53**, 314 (1975).
[18] F. W. Delrio, C. Jaye, D. A. Fischer, and R. F. Cook, Appl. Phys. Lett. **94**, 131909 (2009).
[19] F. J. Blatt, *Thermoelectric Power of Metals* (Plenum, New York, 1976).
[20] L. Shi and A. Majumdar, J. Heat Trans. **124**, 329 (2002).
[21] Y. S. Touloukian and C. Y. Ho, *Thermophysical Properties of Matter* (Plenum, New York 1972), Vols.1 and 2.
[22] C. B. Beetz, Jr., T. A. Perry, and D. T. Morelli, *Science and Technology of New Diamond*, edited by S. Saito, O. Fukunaga, and M. Yoshikawa (Terra Scientific Publishing Company, Tokyo, 1990).
[23] D. Y. Zang and S. R. Forrest, Appl. Phys. Lett. **60**, 189 (1992).
[24] F. Shen, P. Lu, K. H. Lee, T. Y. Ng, and S. J. O'Shea, Sens. Actuators A **95**, 17 (2001).
[25] M. C. Salvadori, A. R. Vaz, F. S. Teixeria, M. Cattani, and I. G. Brown, Appl. Phys. Lett. **88**, 133106 (2006).
[26] M. Cattani, M. C. Salvadori, A. R. Vaz, F. S. Teixeria, and I. G. Brown, J. Appl. Phys. **100**, 114905 (2006).
[27] A. Balduci, M. Marinelli, M. E. Morgada, G. Pucella, G. Rodriguez, M. Scoccia, and G. Verona-Rinati, Microsyst. Technol. **12**, 365 (2006).
[28] I. Chizhov, A. Kahn, and G. Scoles, J. Crystal Growth **208**, 449 (2000).
[29] W. Bohm, T. Fritz, and K. Leo, Phys. Status Solidi A **160**, 81 (1997).
[30] N. Nicoara, E. Roman, J. M. Gomez-Rodriguez, J. A. Martin-Gago, and J. Mendez, Org. Electron. **7**, 287 (2006).
[31] J. B. Neaton, M. S. Hybertsen, and S. G. Louie, Phys. Rev. Lett. **97**, 216405 (2006).